Lepton flavor violation in long-baseline experiments

Joe Sato[a*]

[a]Department of Physics, Faculty of Science, Saitama University,
Shimo Okubo 255, Sakura-ku, Saitama, 338-8570, Japan

We discuss the measurement of new physics in long baseline neutrino oscillation experiments. Through the neutrino oscillation, the probability to detect the new physics effects such as flavor violation is enhanced by the interference with the weak interaction. We carefully explain the situations that the interference can take place. Assuming a neutrino factory and an upgraded conventional beam, we estimate the feasibility to observe new physics numerically and point out that we can search new interactions using some channels, for example $\nu_\mu \to \nu_\mu$, in these experiments. We also discuss the flavor violating effects of Minimal Supersymmetryc Standard Model with right-handed neutrinos in future neutrino oscillation experiments. In this class of models, the effective flavor violating interactions are induced which can interfere with the weak interaction, and show that some new physics effects are large enough to be observed.

1. Introduction

There are many observations of solar neutrino[1], atmospheric neutrino[2], and reactor neutrino[3] showing that neutrinos are massive and hence there is a mixing in lepton sector.

Though neutirnos are massive their masses are very tiny , much smaller than other femions. This fact may suggest that the existence of new physics at very high energy scale, that is, such tiny mass is very well understood by seasaw mechanism[4]. Neutrino experiments also have revealed that lepton mixings are very large, much larger that those of quarks. This indicates that there must be new physics where lepton flavor number is strongly violated.

Therefore we will expect that the nature exhbits those lepton flavor violation (LFV) and hence we may see the remnant of new physics. Indeed, e.g. in Minimal Supersymmetric Standard Model (MSSM) with heavy right-handed neutrinos, charged lepton decay with large lepton flavor violation is expected.[5,6] In this class of models very large lepton flavor violating slepton masses are induced through renormalization due to lepton flavor vviolating couplings.

With the Dirac Neutrino Yukawa couplings,

$$W = f_\nu^{ij} \bar{N}_i L_j H_u, \tag{1}$$

slepton mass remormalization is given by the equation,

$$\begin{aligned} \mu \frac{d(m^2_{\tilde{L}})_{ij}}{d\mu} &= \left(\mu \frac{d(m^2_{\tilde{L}})_{ij}}{d\mu} \right)_{\rm MSSM} (=0) \\ &+ \frac{1}{16\pi^2} \left[m^2_{\tilde{L}} f^\dagger_\nu f_\nu + f^\dagger_\nu f_\nu m^2_{\tilde{L}} \right. \\ &\left. +2(f^\dagger_\nu m^2_{\tilde{\nu}} f_\nu + \tilde{m}^2_{H_u} f^\dagger_\nu f_\nu + A^\dagger_\nu A_\nu) \right]_{ij} . \end{aligned} \tag{2}$$

Here, m^2's are SUSY breaking masses:

$m^2_{\tilde{L}}$	scalar lepton doublet
$m^2_{\tilde{\nu}}$	right-handed sneutrino
$\tilde{m}^2_{H_u}$	doublet Higgs.

A_ν denotes the A-term corresponding to eq. (1). Note that if the Dirac Neutrino Yukawa couplings, eq.(1) do not exist, then there is no LFV effect.

Thus LFV effect can be seen in the second term of R.H.S in eq.(2) where the LFV couplings appear. Approximately this is solved in the following way, with the cutoff M_G and a typical right-handed neutrino scale M_R:

*This work is supported in part by Grants-in-Aid for Scientific Research from the Ministry of Education, Science, Sports, and Culture of Japan, No.14740168 and No.16028202.

$$(\Delta m^2_{\tilde{L}})_{ij} \simeq -\frac{(6+a_0^2)m_0^2}{16\pi^2}(f_\nu^\dagger f_\nu)_{ij}\log\frac{M_G}{M_R}$$
$$\simeq -\frac{(6+a_0^2)m_0^2}{16\pi^2}U^D_{ik}U^{D*}_{jk}|f_{\nu k}|^2\log\frac{M_G}{M_R}\,, \qquad (3)$$
$$U^{D^T} f_\nu^{ij} V^{D^*} \equiv \mathrm{diag}(f_{\nu 1}, f_{\nu 2}, f_{\nu 3})\,,$$

here a_0 is a typical magnitude of the A term.

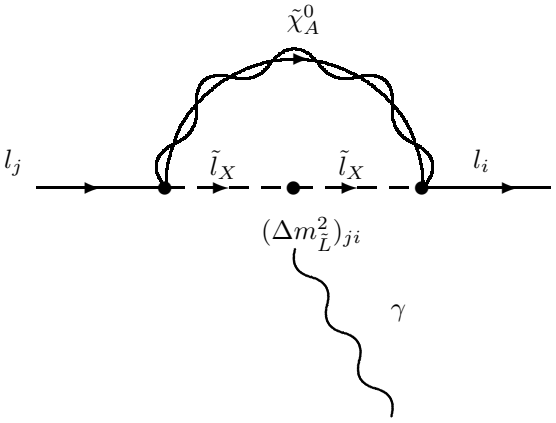

Figure 1. Diagram for Lepton decay with LFV. Approximately this effect is understood by the LFV mass $(\Delta m^w_L)_{ji}(j \neq i)$ term insertion.

We can see that there the off-diagonal element of slepton mass term which is the seed of charged lepton decay with LFV. Graphically this is shown in fig. 1. From this diagram, we see that for $\tau \to \mu\gamma$, $(\Delta m^2_{\tilde{L}})_{32}$ is relevant and for $\mu \to e\gamma$, $(\Delta m^2_{\tilde{L}})_{21}$ is relevant.

The yukawa couplings y_ν^{ij} must be tuned with right-handed neutrino mass matrix so that all the observation can be explained by neutrino oscillations and using such parameters the branching ratios of the charged leptons are calculated.

An example of the branching ratios with appropriate parameters is shown in fig.2. The predicted branching ratio is within a reach of near future experiments[8–10].

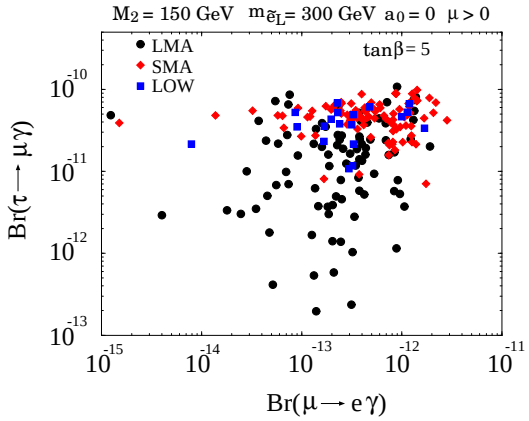

Figure 2. Example of $\mathrm{Br}(\mu \to e\gamma)$ versus $\mathrm{Br}(\tau \to \mu\gamma)$ in a class of models, MSSM with right-handed neutrinos. This is taken from ref.[7].

Then naturally the question whether such an effect can be seen in neutrino oscillation experiments arises. In near future oscillation experiments parameters are expected to be determined very precisely[11,12]. Then since we expect new physics with lepton flavor violation, we would like to ask a question whether we can observe the fragment of such effect in oscillation experiments.

In Sec. 2, we study what we see in long baseline (LBL) neutrino oscillation experiments and parameterize the LFV interactions in such experiments. Next in Sec. 3, we investigate the sensitivity for new physics in future LBL experiments [13–18]. Then in Sec. 4 we calculate how large these new physics effect can be in models of MSSM with right-handed neutrinos. Finally in Sec. 5 we summarize the discussion here.

2. LFV interaction in neutrino oscillation

The basic idea is that the new physics effect appears as an interference with usual oscillation amplitude in oscillation experiments and be "enhanced". To see this concretely let's examine the neutrino factory.[17]

First we note that we do not observe neutrino itself but its product, a corresponding charged

lepton. Neutrino appears only an intermediate state. In a neutrino factory All we know is that the muons, say, with negative charge decay at an accumulate ring and wrong sign muons are observed in a detector located at a length L away just after the time L/c, where c is the light speed. This is depicted schematically in Fig.3.

Since we know that there is the weak interaction process, we interpret such a wrong sign event as the evidence of the neutrino oscillation, $\bar{\nu}_e \to \bar{\nu}_\mu$, which is graphically represented in Fig.4.

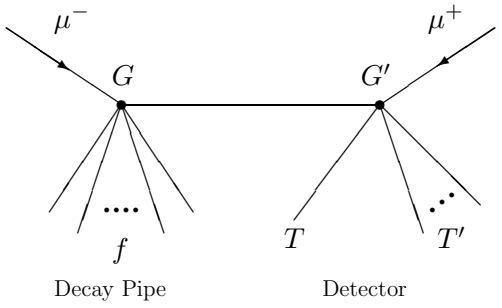

Figure 3. What we really see in a neutrino factory.

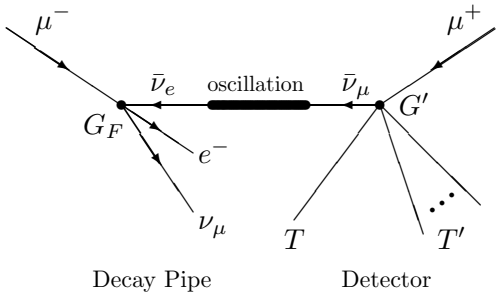

Figure 4. Standard interpretation of a wrong sign event.

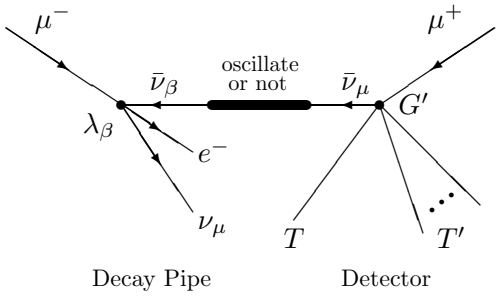

Figure 5. Diagram which gives same signal as that given by Fig.4.

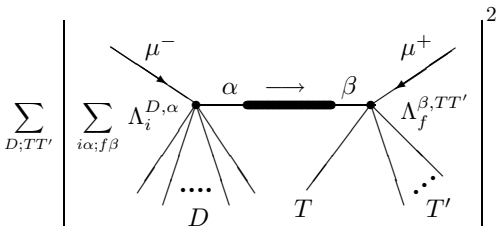

Figure 6. Transition rate for "$\bar{\nu}_e \to \bar{\nu}_\mu$".

Now if there is a flavor-changing exotic interaction, *e.g.*,

$$\lambda(\bar{e}\gamma_\mu\mu)(\bar{\nu_\mu}\gamma^\mu\nu_\alpha), \quad \alpha \neq e, \tag{4}$$

then we will have the same signal of a wrong sign muon, whose diagram is shown in Fig.5, just like that caused by the weak interaction and the neutrino oscillation. We cannot distinguish these two kinds of contribution. The quantum mechanics tells us that in this case, to get a transition rate, we first sum up these amplitudes and then square the summation. Therefore there is an interference phenomenon between several amplitudes in this process.

To estimate the transition probability for $\bar{\nu}_e \to \bar{\nu}_\mu$, we have to calculate the diagram depicted in fig. 6.

The usual oscillation term, fig.4 must give the leading contribution and we expand the graph, 6,

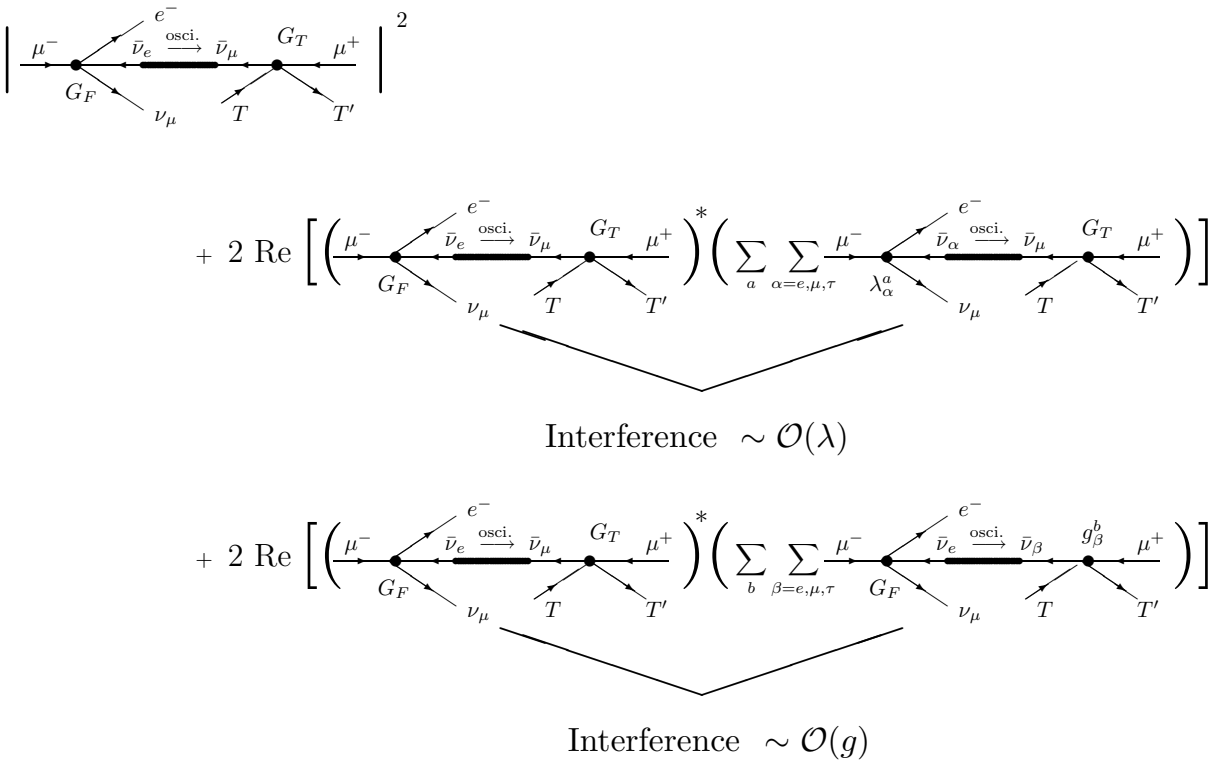

Figure 7. The transition probability of a wrong-sign muon appearance process up to sub-leading contribution.

into the form of fig. 7. (Here the graph representing flavor changing propagation effect is omitted.)

Note that the transition probability depends on not quadratically but linearly new physics couplings. To estimate those effect we need to parameterize their effect in the framework of neutrino oscillation.

The amplitude for "neutrino oscillation" can be divided into three pieces: (1) Amplitude relevant with decay of a parent particle denoted as A^C_α, here C describes the type of interactions. For μ decay, as we will see in eq.(6) and (7), there are two types of interactions, $C = L, R$ while for π decay we do not need this label. α distinguishes the particle species which easily propagates in the matter and make an interaction at a detector. (2) Amplitude representing a transition of these propagating particles, which are usually neutrinos, from one species α to another/same β, denoted as $T_{\alpha\beta}$. (3) Amplitude responsible for producing a charged lepton l from a propagated particle β at a detector, stood for by $D^I_{\beta l}$. Here I denotes an interaction type. Using these notations we get the probability to observe a charged lepton $l^\pm$ at a detector as

$$P_{\mu^- \to l^+(l^-)} = \left| \sum_{\alpha\beta CI} A^C_\alpha T_{\alpha\beta} D^I_{\beta l^\pm} \right|^2$$
$$= \sum_{\alpha\beta CI} \sum_{\alpha'\beta' C' I'} A^C_\alpha T_{\alpha\beta} D^I_{\beta l^\pm} A^{C'*}_{\alpha'} T^*_{\alpha'\beta'} D^{I'*}_{\beta' l^\pm}. \quad (5)$$

Therefore we can consider the effect of new physics separately for decay, propagation and detection processes.

First we consider the decay process of parent particles. Since all final states must be the same,

for a neutrino factory, the exotic decays of muons which are $\mu^- \to e^- \nu_\alpha \bar{\nu}_e$ and $\mu^- \to e^- \nu_\mu \bar{\nu}_\beta$ can be amplified by the interference. Though in the presence of Majorana mass terms neutrinos and anti neutrinos can mix with each other, this effect is strongly suppressed by m_ν/E_ν. Therefore we do not have to consider decays into neutrino with opposite chirality such as $\mu^- \to e^- \bar{\nu}_\mu \bar{\nu}_\beta$ The former is relevant with $\mu^- \to l^-$ and the latter is relevant with $\mu^- \to l^+$. In other words, we can approximate neutrinos to be massless except for the propagation process. This fact and Lorentz invariance allow only two kinds of new interactions in this process. For a wrong-sign mode, the allowed two interactions are the $(V-A)(V-A)$ type,

$$2\sqrt{2}\lambda_\alpha(\bar{\nu_\mu}\gamma^\rho P_L \mu)(\bar{e}\gamma_\rho P_L \nu_\alpha), \quad \alpha = \mu, \tau, \tag{6}$$

which has the same chiral property as the weak interaction but violates the flavor conservation, and the $(V-A)(V+A)$ type,

$$2\sqrt{2}\lambda'_\alpha(\bar{\nu_\mu}\gamma^\rho \nu_\alpha)(\bar{e}\gamma_\rho P_R \mu), \quad \alpha = e, \mu, \tau. \tag{7}$$

The latter has different chiral property from the former, so that it gives different energy dependence to the transition rate. These exotic interactions interfere with the leading amplitude and contribute as next leading effects. Note that generally λ and λ' are complex numbers.[13]

In the case of the $(V-A)(V-A)$ type exotic interaction, we can introduce the interference effect by treating the initial state of oscillating neutrino as the superposition of all flavor eigenstates. On the $\mu^- \to \mu^+$ process, we can take initial neutrino $\bar{\nu}$ as

$$\bar{\nu} = \bar{\nu}_e + \epsilon_\mu \bar{\nu}_\mu + \epsilon_\tau \bar{\nu}_\tau, \tag{8}$$

where $\epsilon_\alpha = \lambda_\alpha / G_F$. This simple treatment is allowed only for the $(V-A)(V-A)$ type interaction because of the same interaction form as the weak interaction except for difference of the coupling constant and the flavor of antineutrino. In this case we can generalize the initial neutrino for any flavor, using Y. Grossman's source state notation [19], as, [2]

$$\nu^s_\beta = U^s_{\beta\alpha}\nu_\alpha, \quad \alpha, \beta = e, \mu, \tau,$$

$$U^s \equiv \begin{pmatrix} 1 & \epsilon^s_{e\mu} & \epsilon^s_{e\tau} \\ \epsilon^s_{\mu e} & 1 & \epsilon^s_{\mu\tau} \\ \epsilon^s_{\tau e} & \epsilon^s_{\tau\mu} & 1 \end{pmatrix}. \tag{9}$$

We can include the total exotic effect into the oscillation probability as

$$P_{\nu^s_\alpha \to \nu_\beta} = \left| \langle \nu_\beta | e^{-iHL} U^s_{\alpha\gamma} | \nu_\gamma \rangle \right|^2. \tag{10}$$

This treatment is also valid for the effect on the ν_μ oscillation.

In the case of the $(V-A)(V+A)$ type exotic interaction, we cannot treat interference terms simply. The interference term between the weak interaction and an exotic interaction eq.(7) denoted as $P^{(1)}_{\mu\to l}$ gives the rate for the observation of the wrong sign charged lepton, which is interpreted normally as the oscillation from $\bar{\nu}_e \to \bar{\nu}_l$ in μ^- decay, as follows:

$$\begin{aligned} & P^{(1)}_{\mu^- \to l^+} \\ = \; & \frac{1+\mathcal{P}_\mu}{2} \frac{1}{(2\pi)^2} \\ & \times \sum_{\text{spin}} \int \frac{d^3p_e}{2E_e} \frac{d^3p_{\nu_\mu}}{2E_{\nu_\mu}} \delta^4(p_\mu - p_{\bar{\nu}} - p_e - p_{\nu_\mu}) \\ & \times 2\text{Re}\left[A^{L*}_e \sum_{\beta I} T^*_{e\beta} D^{I*}_{\beta l^+} \sum_{\alpha\beta' I'} A^R_\alpha T_{\alpha\beta'} D^{I'}_{\beta' l^+} \right] \\ = \; & \frac{1+\mathcal{P}_\mu}{2} \frac{8G_F}{\pi} m_e m_\mu E_\nu (|\mathbf{p}_\mu| - E_\mu) \\ & \times \sum_{\alpha\beta\beta' II'} \text{Re}[\lambda'_\alpha T^*_{e\beta} D^{I*}_{\beta l^+} T_{\alpha\beta'} D^{I'}_{\beta' l^+}], \end{aligned} \tag{11}$$

where $\mathcal{P}_\mu$ is the polarization of the initial μ^-, E_ν is ν energy, and $\mathbf{p}_\mu(E_\mu)$ is μ momentum (energy).

In the case for the observation of the same sign charged lepton, which is interpreted as the oscillation from $\nu_\mu \to \nu_l$ in μ^- decay, as follows:

$$\begin{aligned} P^{(1)}_{\mu^- \to l^-} &= \frac{1-\mathcal{P}_\mu}{2} \frac{8G_F}{\pi} m_e m_\mu E_\nu (|\mathbf{p}_\mu| - E_\mu) \\ &\times \sum_{\alpha\beta\beta' II'} \text{Re}[\lambda'_\alpha T^*_{\mu\beta} D^{I*}_{\beta l^-} T_{\alpha\beta'} D^{I'}_{\beta' l^-}], \end{aligned} \tag{12}$$

For π decay the situation is much simpler. In the presence of new physics there may be a flavor violating decay of π such as $\pi^- \to \mu^- \nu_\alpha (\alpha = e, \tau)$. This effect changes the initial ν state;

$$\nu_\mu \longrightarrow \nu^s_\mu = \epsilon^s_{\mu e}\nu_e + \nu_\mu + \epsilon^s_{\mu\tau}\nu_\tau. \tag{13}$$

[2] U^s is not necessarily unitary.

In this case we do not have to worry about the type of new physics which gives a flavor changing π decay at a low energy scale. Due to kinematics, the energy and the helicity of the decaying particles, μ and ν are fixed.

Next we consider the propagation process. Exotic interactions also modify the Hamiltonian for neutrino propagation as [14],

$$H_{\beta\alpha} = \frac{1}{2E_\nu}\left\{ U_{\beta i}\begin{pmatrix} 0 & & \\ & \delta m^2_{21} & \\ & & \delta m^2_{31} \end{pmatrix} U^\dagger_{i\alpha} + \begin{pmatrix} \bar{a}+a_{ee} & a_{e\mu} & a_{e\tau} \\ {a_{e\mu}}^* & a_{\mu\mu} & a_{\mu\tau} \\ {a_{e\tau}}^* & {a_{\mu\tau}}^* & a_{\tau\tau} \end{pmatrix}_{\beta\alpha} \right\}, \quad (14)$$

where $\bar{a}$ is the ordinary matter effect given by $2\sqrt{2}G_F n_e E_\nu$, $a_{\alpha\beta}$ is the extra matter effect due to new physics interactions, that is defined by $a_{\alpha\beta} = 2\sqrt{2}\epsilon^m_{\alpha\beta}G_F n_e E_\nu$. Note that to consider the magnitude of the matter effect, the type of the interaction is irrelevant since in matter particles are at rest and hence the dependence on the chirality is averaged out.[20]

Finally we make a comment about new physics which affect a detection process. To consider this process we need the similar treatment to that at the decay process, that is, we have to separate contribution of new interactions following the difference of the chirality dependence. However to take into account new physics at a detector, the parton distribution and a knowledge about hadronization are necessary. Though we may wonder whether we can parameterize the effect of new physics at the detector g/G_T as ϵ^d like ϵ^s. It is expected that ϵ^d has a complicated energy dependence due to the parton distribution for example in a energy region of a neutrino factory. Consider the case that there is an elementary process from lepton flavor violating new physics including strange quark. To parameterize its effect we need both its magnitude and the distribution function of strange quark in nucleon which will show the dependence on the neutrino energy (more exactly, the transfered momentum from neutrino to strange quark). They are beyond our ability and hence we do not consider them further in this paper, though new physics which can affect the decay process have contribution to the detection process too.

3. Model independent reach

3.1. Explanation of Numerical Analysis

For a neutrino factory, we use following procedures: First, we assume the magnitude of the effects caused by new interactions. Next, we calculate the event numbers including the effects of new physics N^{NP} and also calculate that based on the standard model N^{SM}. Then, we define the following quantity, so called χ^2 function [3],

$$\chi^2 \equiv \sum_i^{\text{bin}} \frac{\left|N_i^{NP} - N_i^{SM}\right|^2}{N_i^{SM}} \equiv N_\mu M_{\text{det}} X^2_{\nu-\text{fact}}, \quad (15)$$

where i is the energy bin index, N_μ is the muon number, and M_{det} is the detector mass. To claim that new physics effects can be observed at 90% confidence level, it is required

$$\chi^2 > \chi^2_{90\%}, \quad (16)$$

and this condition is rewritten as

$$N_\mu M_{\text{det}} > \frac{\chi^2_{90\%}}{X^2_{\nu-\text{fact}}}. \quad (17)$$

From the above method, we can obtain the necessary muon number and the detector mass to observe the new physics effects at 90% confidence level.

On the other hand, there are some kinds of option on beam configurations for an upgraded conventional beam; wide band, narrow band, off axis, and so on. We discuss the event number of *no-oscillated neutrino events* at the detector N_ν unlike the case for a neutrino factory. The concrete procedure is almost the same as that for a neutrino factory. We separate χ^2 function defined

[3] Strictly speaking, this quantity is "power of test" to distinguish two theories, the theory including new physics and the standard model. Furthermore, note that since we are interested in "goodness of fit" for two theories, we should compare this quantity with χ^2 distribution function with one degree of freedom. More detail on statistics is found in Ref.[21].

in first line of eq.(15) into two parts;

$$\chi^2 \equiv N_\nu X^2_{\rm conv}, \tag{18}$$

and get the necessary number of no-oscillated neutrino events from

$$N_\nu > \frac{\chi^2_{90\%}}{X^2_{\rm conv}}. \tag{19}$$

In the numerical calculation for a conventional beam, we consider the wide-band-beam like situation, whose flux distribution for energy is constant.

3.2. $(V-A)(V-A)$ type new interaction

Here, we deal with the case that there are only $(V-A)(V-A)$ type new interactions in the lepton sector. In this case, we need to consider the effect represented in eqs.(9) and (14). Before making the presentation of the numerical calculations, we give the analytic expression for the sensitivities to understand the essential features. As we showed in section III, the interference terms between $(V-A)(V-A)$ type interactions and the weak interaction have the same dependence on the μ polarization leading term does. It can not be expected that the sensitivity to such interference term becomes better by the control of the parent μ polarization. We consider here an unpolarized muon beam. The "oscillation probability" is given by eq.(10) in this situation. More detailed calculations are presented in the Appendix of [17].

3.2.1. $\nu_e \to \nu_\mu$ channel in a neutrino factory

The analytic expression of probability for $\nu_e \to \nu_\mu$ given in the Appendix of [17] shows that the effect due to $\epsilon^m_{\mu\tau}$ and $\epsilon^{s,m}_{\alpha\alpha}$ are irrelevant since these terms are proportional to $\sin^2 2\theta_{13} \times \epsilon$ in the high energy region, so it is difficult to observe their effects. The flavor changing processes between muon and electron, *e.g.,* $\mu \to e\gamma$, $\mu \leftrightarrow e$ conversion, are strictly constrained from experiments, and as we argue in the next section the box diagrams of the μ-to-e processes must relate to $\epsilon^s_{e\mu}$ and $\epsilon^s_{\mu e}$. Therefore, the magnitude of $\epsilon^s_{e\mu}$ has very severe bound and the terms depending on it are also not effective. Assuming some models, *e.g.*, MSSM with right-handed neutrinos, it is expected that the magnitude of $\epsilon^s_{\alpha\beta}$ and $\epsilon^m_{\alpha\beta}$ are the same order because they are produced by similar diagrams. This is also discussed in the next section. We assume naively that the terms depending on $\epsilon^m_{e\mu}$ are constrained as $\epsilon^s_{e\mu}$. On the other hand, the τ-to-e processes do not give the tight bound to $\epsilon^{s,m}_{e\tau}$. Hence, we investigate the effect induced by $\epsilon^{s,m}_{e\tau}$ first.

Before surveying the required $N_\mu M_{\rm det}$ for each baseline L and muon energy E_μ, we see the behavior of contribution of $\epsilon^{s,m}_{e\tau}$ to the "oscillation probability" to consider the optimum setup for L and E_μ. In the high energy region such as the matter effect $\bar{a}$ is much greater than δm^2_{31}, the first order contribution of $\epsilon^{s,m}_{e\tau}$ to the transition probability, $\Delta P_{\nu_e\to\nu_\mu}\{\epsilon_{e\tau}\}$, is constructed by four parts that have the different $\epsilon^{s,m}_{e\tau}$ dependences:

$$\Delta P_{\nu_e\to\nu_\mu}\{\epsilon_{e\tau}\} = 2 s_{23} s_{2\times 23} s_{2\times 13}$$

$$\times \left[c^2_{13} \left(s_\delta {\rm Re}[\epsilon^s_{e\tau}] - c_\delta {\rm Im}[\epsilon^s_{e\tau}]\right) \left(\frac{\bar{a}}{4E_\nu} L\right) \left(\frac{\delta m^2_{31}}{4E_\nu} L\right)^2 \right. \tag{20a}$$

$$+ c^2_{13} \left(c_\delta {\rm Re}[\epsilon^s_{e\tau}] + s_\delta {\rm Im}[\epsilon^s_{e\tau}]\right) \left\{ 1 - \frac{1}{2}\left(\frac{\bar{a}}{4E_\nu} L\right)^2 \right.$$

$$\left. \left. - s^2_{13} \left(\frac{\bar{a}}{4E_\nu} L\right) \left(\frac{\delta m^2_{31}}{4E_\nu} L\right) \right\} \left(\frac{\delta m^2_{31}}{4E_\nu} L\right)^2 \right. \tag{20b}$$

$$\left. - c^2_{13} \left(s_\delta {\rm Re}[\epsilon^m_{e\tau}] + c_\delta {\rm Im}[\epsilon^m_{e\tau}]\right) \left(\frac{\bar{a}}{4E_\nu} L\right) \left(\frac{\delta m^2_{31}}{4E_\nu} L\right)^2 \right. \tag{20c}$$

$$\left. - \frac{1}{3} s^2_{13} \left(c_\delta {\rm Re}[\epsilon^m_{e\tau}] - s_\delta {\rm Im}[\epsilon^m_{e\tau}]\right) \left\{ \left(\frac{\bar{a}}{4E_\nu} L\right) \right. \right.$$

$$\left. \left. + 2\left(\frac{\delta m^2_{31}}{4E_\nu} L\right) \right\} \left(\frac{\bar{a}}{4E_\nu} L\right) \left(\frac{\delta m^2_{31}}{4E_\nu} L\right)^2 \right], \tag{20d}$$

where $s_{2\times ij} \equiv \sin 2\theta_{ij}$. Since we can suppose that E_ν is proportional to E_μ in a neutrino factory, E_μ and L dependence of the sensitivity to each term can be approximated as

$$\chi^2({\rm 20b}) \propto \left\{ 1 - \frac{1}{2}\left(\frac{\bar{a}}{4E_\mu} L\right)^2 \right\}^2 \times E_\mu,$$

$$\chi^2({\rm 20a, 20c}) \propto \left(\frac{\bar{a}}{4E_\mu} L\right)^2 \times E_\mu,$$

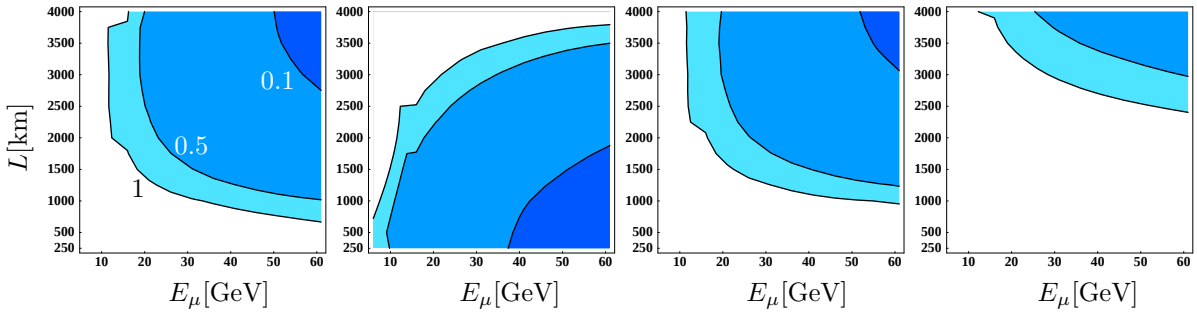

Figure 8. Contour plots of the required $N_\mu M_{\rm det}$ to observe the new physics effects concerning $\epsilon^{s,m}_{e\tau}$ at 90% C.L. in $\nu_e \to \nu_\mu$ channel using a neutrino factory. From left to right: $(\epsilon^s_{e\tau}, \epsilon^m_{e\tau}) = (3.0\times10^{-3}, 0)$, $(3.0\times10^{-3}i, 0)$, $(0, 3.0\times10^{-3})$, $(0, 3.0\times10^{-3}i)$. The uncertainties of theoretical parameters are not considered in these plots. As we point out in the text, when the uncertainties are taken into account, the sensitivities are completely lost. In Fig.8 to Fig.14, contours mean 0.01, 0.05, 0.1, 0.5, $1\times10^{21}\cdot 100$kt.

$$\chi^2(20\mathrm{d}) \propto \left(\frac{\bar{a}}{4E_\mu}L\right)^4 \times E_\mu. \tag{21}$$

All of eq.(21) are proportional to E_μ, so the sensitivities must get better as the energy becomes higher.

Each of eq.(21) depends on L in different way. χ^2(20b) become tiny for longer baseline length within the region that we are now interested in. This fact means that a shorter baseline experiment has an advantage over a longer one to observe (20b)'s effect. In contrast with this, it is found that longer baseline will be better to search for the effects of (20a), (20c) and (20d).

Each of eq.(21) depends on the combinations of $\epsilon^{s,m}_{e\tau}$ and the CP phase δ. What we observe is the combination of them. The effects of ϵ's can be sources of the CP-violation effect.[13] In the discussion about the observation of the CP phase, this fact should be considered. The analytic expressions also show that the sensitivities are proportional to $|\epsilon|^2$.

Now, we show the results of the numerical calculations. The parameters that we use here are

$$\sin\theta_{12} = \frac{1}{2}, \quad \sin\theta_{23} = \frac{1}{\sqrt{2}}, \quad \sin\theta_{13} = 0.1,$$
$$\delta m^2_{21} = 5\times10^{-5}, \quad \delta m^2_{31} = 3\times10^{-3}, \tag{22}$$
$$\delta = \frac{\pi}{2},$$

and take $|\epsilon| = 3\times10^{-3}$, which is a reference value for the feasibility to observe the effect by using the method of the oscillation enhancement. Except for $\epsilon^{s,m}_{e\mu}$ and $\epsilon^s_{\mu e}$, the constraints of the processes of charged lepton have not forbidden this magnitude of ϵ's.

Fig.8 shows the required $N_\mu M_{\rm det}$ in the case where we do not take into account the uncertainties of the mixing parameters. We can check whether the approximated equations, eq.(21), are correct from the behavior of the plots. As eq.(20) implies, contribution from the new interaction depends on the combinations of ϵ and δ. We take $\delta = \pi/2$, so we can extract each term of eq.(20) by taking $\epsilon^{s,m}_{e\tau}$ pure real and imaginary. Therefore, the plots of Fig.8 from left to right correspond to the required data size to observe each term in eq.(20a) to eq.(20d) respectively. The behavior of these plots is consistent with the expectations from the analytic expressions in eq.(21). To consider realistic situations, the new physics effects in both source and matter must be taken into account simultaneously. The total effects are given by the simple summation of each effect.

In realistic situations the uncertainties of the theoretical parameters have to be taken into ac-

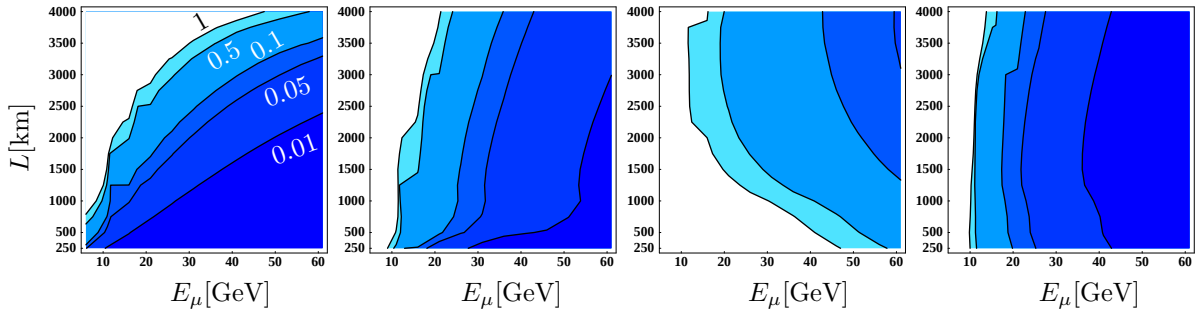

Figure 9. Contour plots of the required $N_\mu M_{\rm det}$ to observe the new physics effects concerning $\epsilon^{s,m}_{e\mu}$ at 90% C.L. in $\nu_e \to \nu_\mu$ channel when there is no uncertainty for theoretical parameters. From left to right: $(\epsilon^s_{e\mu}, \epsilon^m_{e\mu}) = (3.0\times10^{-3}, 0)$, $(3.0\times10^{-3}i, 0)$, $(0, 3.0\times10^{-3})$, $(0, 3.0\times10^{-3}i)$. Each plot corresponds to the sensitivities to eq.(24a)$\sim$eq.(24d) respectively.

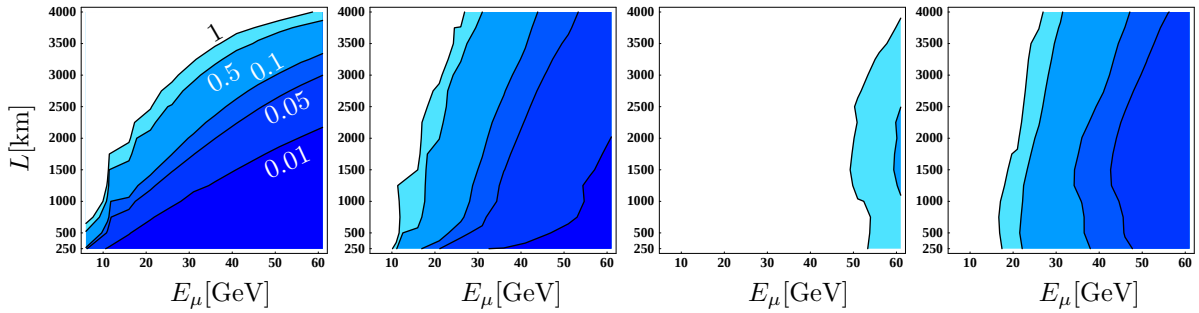

Figure 10. Same as Fig.9, but here each parameter has 10% uncertainty.

count.[4] Once the uncertainties are introduced, it can be expected that the sensitivities shown in Figs.8 will be spoiled completely. The $\epsilon^{s,m}_{e\tau}$ effect can be absorbed easily into the main (unperturbed) part of oscillation,

$$s^2_{23}s^2_{2\times13}\left(\frac{\delta m^2_{31}}{4E_\nu}L\right)^2, \tag{23}$$

by adjusting the theoretical parameters since the effects have the same energy dependence as the main part has. Indeed, taking into account these uncertainties, the sensitivities to $\epsilon^{s,m}_{e\tau}$ are completely washed out. Therefore, we have to look for the terms whose energy dependence differ from that of the main oscillation term in the high energy region. In $\nu_e \to \nu_\mu$ channel, the effects caused by $\epsilon^{s,m}_{e\mu}$ have such energy dependence. It can be represented analytically in the high energy region as

$$\begin{aligned}\Delta P_{\nu^s_e\to\nu_\mu}\{\epsilon_{e\mu}\} &= 2s_{23}s_{2\times13}\\ &\times\left[\left(s_\delta{\rm Re}[\epsilon^s_{e\mu}] - c_\delta{\rm Im}[\epsilon^s_{e\mu}]\right)\times\left\{1-\frac{2}{3}\left(\frac{\bar a}{4E_\nu}L\right)^2\right.\right.\\ &\left.\left.+\frac{2}{3}\left(2c_{2\times13}-3c^2_{23}c^2_{13}\right)\left(\frac{\bar a}{4E_\nu}L\right)\left(\frac{\delta m^2_{31}}{4E_\nu}L\right)\right\}\left(\frac{\delta m^2_{31}}{4E_\nu}L\right)\right.\end{aligned} \tag{24a}$$

[4] We understand that systematic errors should be also taken into account. However in this paper we refer to the errors originated from statistics and we treat the errors in the theoretical parameters.

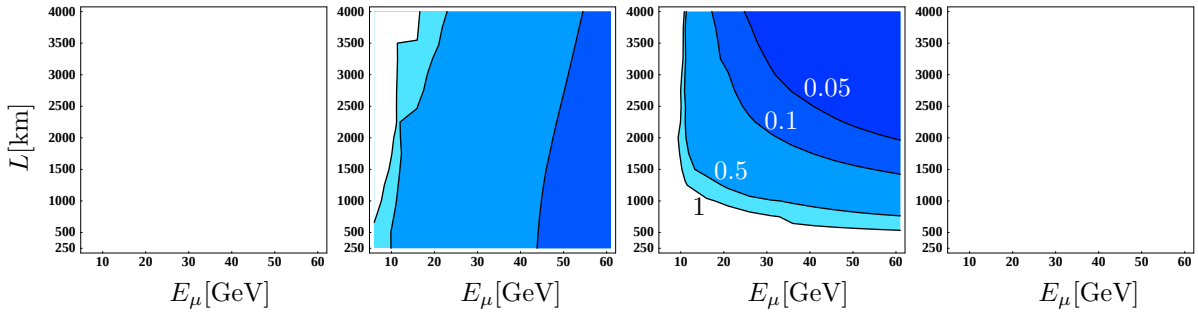

Figure 11. Contour plots of the required $N_\mu M_{\rm det}$ to observe the new physics effects concerning $\epsilon^{s,m}_{\mu\tau}$ at 90% C.L. in $\nu_\mu \to \nu_\mu$ channel. All theoretical parameters are assumed to have 10% uncertainty. From left to right, each plot corresponds to $(\epsilon^s_{\mu\tau}, \epsilon^m_{\mu\tau}) = (3.0\times10^{-3}, 0)$, $(3.0\times10^{-3}i, 0)$, $(0, 3.0\times10^{-3})$, $(0, 3.0\times10^{-3}i)$. "White Graphs" indicate that there is no sensitivity for the corresponding parameters.

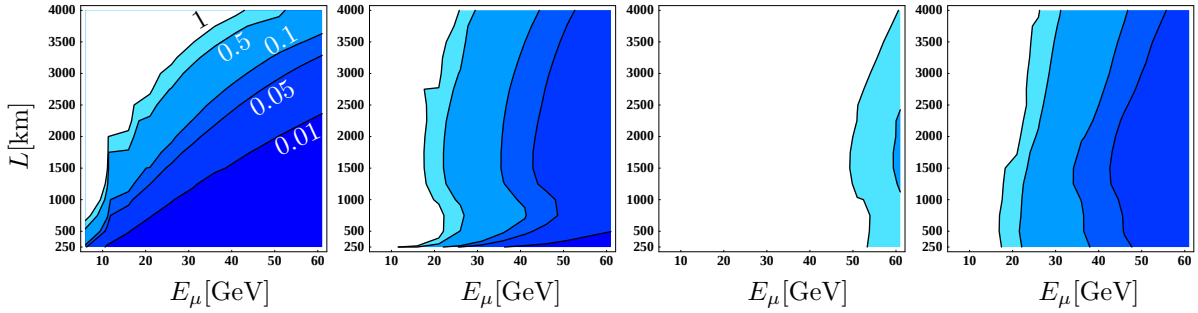

Figure 12. Contour plots of the required $N_\mu M_{\rm det}$ to observe the new physics effects concerning $\epsilon^{s,m}_{e\tau}$ at 90% C.L. in $\nu_e \to \nu_\tau$ channel. All theoretical parameters are assumed to have 10% uncertainty. From left to right, each plot corresponds to $(\epsilon^s_{e\tau}, \epsilon^m_{e\tau}) = (3.0\times10^{-3}, 0)$, $(3.0\times10^{-3}i, 0)$, $(0, 3.0\times10^{-3})$, $(0, 3.0\times10^{-3}i)$.

$$
\begin{aligned}
&- \left(c_\delta \mathrm{Re}[\epsilon^s_{e\mu}] + s_\delta \mathrm{Im}[\epsilon^s_{e\mu}]\right) \\
&\times \left[\left\{1 - \frac{1}{3}\left(\frac{\bar{a}}{4E_\nu}L\right)^2\right\}\left(\frac{\bar{a}}{4E_\nu}L\right)\right. \\
&- \left\{1 - 2s^2_{23}c^2_{13} - \left(1 - c^2_{13}\left(2 - \frac{4}{3}c^2_{23}\right)\right)\right. \\
&\left.\left.\times \left(\frac{\bar{a}}{4E_\nu}L\right)^2\right\}\left(\frac{\delta m^2_{31}}{4E_\nu}L\right)\right]\left(\frac{\delta m^2_{31}}{4E_\nu}L\right) \qquad (24b) \\
&+ 2c^2_{23}\left(s_\delta \mathrm{Re}[\epsilon^m_{e\mu}] + c_\delta \mathrm{Im}[\epsilon^m_{e\mu}]\right)\left(\frac{\bar{a}}{4E_\nu}L\right)\left(\frac{\delta m^2_{31}}{4E_\nu}L\right)^2 \qquad (24c)
\end{aligned}
$$

$$
\begin{aligned}
&+ 2\left(c_\delta \mathrm{Re}[\epsilon^m_{e\mu}] - s_\delta \mathrm{Im}[\epsilon^m_{e\mu}]\right)\left\{1 - \frac{1}{3}\left(\frac{\bar{a}}{4E_\nu}L\right)^2\right. \\
&\left.+ \left(c^2_{23}s^2_{13} + \frac{2}{3}s^2_{23}c_{2\times13}\right)\left(\frac{\bar{a}}{4E_\nu}L\right)\left(\frac{\delta m^2_{31}}{4E_\nu}L\right)\right\} \\
&\left(\frac{\bar{a}}{4E_\nu}L\right)\left(\frac{\delta m^2_{31}}{4E_\nu}L\right)\Bigg]. \qquad (24d)
\end{aligned}
$$

Contribution for the transition probability labeled (24a), (24b) and (24d) depends on $1/E_\mu$. Consequently, the sensitivities to the terms must be robust against the uncertainties of the theoretical parameters since in the high energy region they can be distinguished from the main oscil-

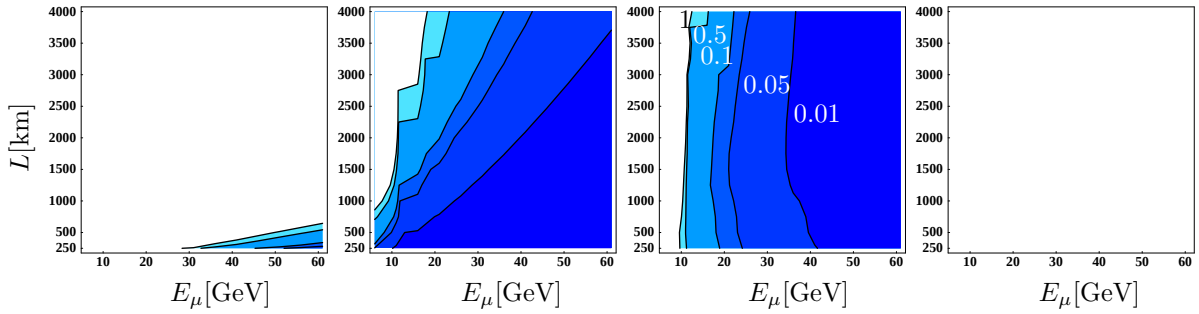

Figure 13. Same as Fig.11, but $\nu_\mu \to \nu_\tau$ channel.

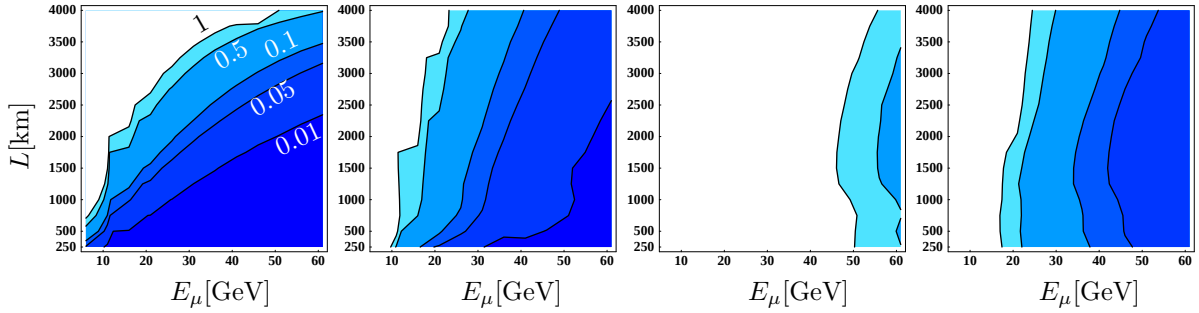

Figure 14. Contour plots of the required $N_\mu M_{\rm det}$ to observe the new physics effects concerning $\epsilon^s_{\mu e}$ and $\epsilon^m_{e\mu}$ at 90% C.L. in $\nu_\mu \to \nu_e$ channel. All theoretical parameters are assumed to have 10% uncertainty. From left to right, each plot corresponds to $(\epsilon^s_{\mu e}, \epsilon^m_{e\mu}) = (3.0\times10^{-3}, 0)$, $(3.0\times10^{-3}i, 0)$, $(0, 3.0\times10^{-3})$, $(0, 3.0\times10^{-3}i)$.

lation part by observing the energy dependence. The claims mentioned above are confirmed numerically by Fig.9 and 10. By comparison of these graphs, we can see that the sensitivities to observe the contribution of (24a), (24b) and (24d) do not suffer from the uncertainties.[5] Incidentally, we note that though the uncertainties wreck the sensitivity to (24c) since it is proportional to $1/E_\mu^2$, the $\epsilon^m_{e\mu}$ second order term brings constant contribution for energy and this signal does not vanish.

[5]To clarify the statement here we adopt large values for $\epsilon^{s,m}_{e\mu}$. The value of $\epsilon_{e\mu}$ in Fig.9 and 10 are too large to avoid the current experimental bound. As we said first, $\epsilon^{s,m}_{e\mu}$ are bound so strictly that these terms can not be observed.

3.2.2. $\nu_\mu \to \nu_\mu$ channel in a neutrino factory

Only the effect that depend on $\epsilon^{s,m}_{\mu\tau}$ will be large enough to be observed in $\nu_\mu \to \nu_\mu$ disappearance channel. As we show in the next section, this quantity is not strongly bound by the charged lepton processes. The analytic expressions for the terms concerning $\epsilon^{s,m}_{\mu\tau}$ (see the Appendix of [17]) indicate two facts: (1) this channel sensitive only to the real part of $\epsilon^m_{\mu\tau}$, and (2) the effect that comes from the real part of $\epsilon^s_{\mu\tau}$ will be small in the assumed parameter region. In addition, it shows that the terms depending on $\epsilon^{s,m}_{\mu\tau}$ are hard to be absorbed by the uncertainty of the theoretical parameters. Note that these terms do not depend on the CP phase δ, that is, it is expected that we can get information on the phases of $\epsilon^{s,m}_{\mu\tau}$. The

sensitivity plots calculated numerically are shown in Fig.11. They behave as expected by the analytic expressions. The uncertainties of the theoretical parameters do not affect the sensitivity since the terms that depend on $1/E_\mu$ do not vanish in the high energy region. The sensitivities depend strongly on the phase of $\epsilon^{s,m}_{\mu\tau}$ but do not depend on δ. We can directly know the phase of the lepton-flavor violation process without care of δ.

3.2.3. Channels with τ and e observation in a neutrino factory

The technologies for tau observation in ν_τ detection [22] and the charge identification of electron to distinguish ν_e with $\bar{\nu}_e$ [23] are under R & D. If it is possible to observe these particles clearly, what can we get ?

In $\nu_e \to \nu_\tau$ channel, we can explore $\epsilon^{s,m}_{e\tau}$ (see Fig.12). The uncertainties of the theoretical parameters will not disturb the sensitivity. In $\nu_\mu \to \nu_\tau$ channel, all we can observe is only the effect of $\epsilon^{s,m}_{\mu\tau}$ (see Fig.13). In comparison with $\nu_\mu \to \nu_\mu$ channel, we will not have so much benefit in terms of sensitivities to the magnitude of ϵ.[6] However in this channel unlike $\nu_\mu \to \nu_\mu$ channel, the observable must depend on the combination of the $\epsilon^{s,m}_{\mu\tau}$'s phase and the CP phase δ, that is, the observation in these two channels are qualitatively different. In $\nu_\mu \to \nu_e$ channel, we can search the effect of not $\epsilon^s_{e\mu}$ but $\epsilon^s_{\mu e}$ at the muon decay process and the effect of $\epsilon^m_{e\mu}$ at the propagation process just like $\nu_e \to \nu_\mu$ channel (see Fig.14). In $\nu_e \to \nu_e$ disappearance channel, oscillation effects themselves are much smaller than the no-oscillation signal. Though some effects of new physics give the different energy dependence from the main oscillation term, we will not be able to get any information for oscillation-enhanced new physics.

3.3. Short Summary

Here we give a short summary for this section. For $(V-A)(V-A)$ interaction type in neutrino factories,

■ In $\nu_\alpha \to \nu_\beta$, the effects induced by $\epsilon^{s,m}_{\alpha\beta}$ will be well observed. The others are too small or easy to be absorbed into the error of the oscillation parameters.

■The expected sensitivity is $\epsilon \gtrsim \mathcal{O}(10^{-4})$.

	$\epsilon^{s,m}_{e\mu}(\epsilon^s_{\mu e})$	$\epsilon^{s,m}_{e\tau}$	$\epsilon^{s,m}_{\mu\tau}$
$\nu_e \to \nu_\mu$	△	△	×
$\nu_\mu \to \nu_\mu$	×	×	◯
$\nu_e \to \nu_\tau$	×	◯	△
$\nu_\mu \to \nu_\tau$	×	△	◯
$\nu_\mu \to \nu_e$	△	×	×
$\nu_e \to \nu_e$	×	×	×

Model-independently we can obtain the constraint on ϵ's from SU(2) inverted process[19]. For example, the constraint on $\mu^- \to e^-\nu_\tau\bar{\nu}_e$ can be obtained from the process $\tau^- \to \mu^- e^- e^+$. Thus naively, we get constraints, say for ϵ^s's, as follows: $\epsilon^s_{e\tau} \lesssim 3.1 \times 10^{-3}$, $\epsilon^s_{e\mu} \lesssim 5 \times 10^{-5}$, $\epsilon^s_{\mu\tau} \lesssim 3.2 \times 10^{-3}$. Factor 2-3[17] or maybe 10[15] could be multiplied on these constraint since SU(2) is broken.

4. MSSM with right-handed neutrinos

Similarly to the effect of $\mu \to e\gamma$, we can draw diagrams which indicate the LFV processes including neutrinos. Examples of LFV interaction in muon decay are given in the following diagrams.

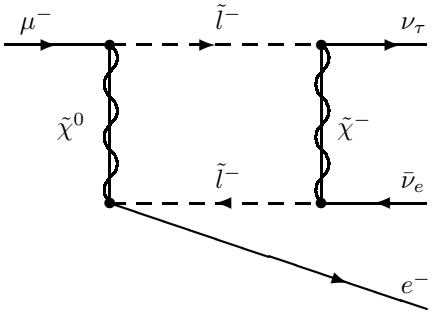

[6]Including systematic errors we will have much benefit.

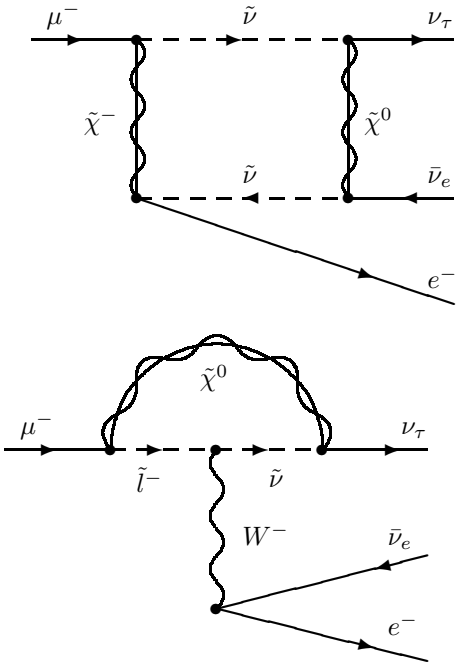

Similarly, examples of LFV interactions in matter effect are given in the following diagrams.

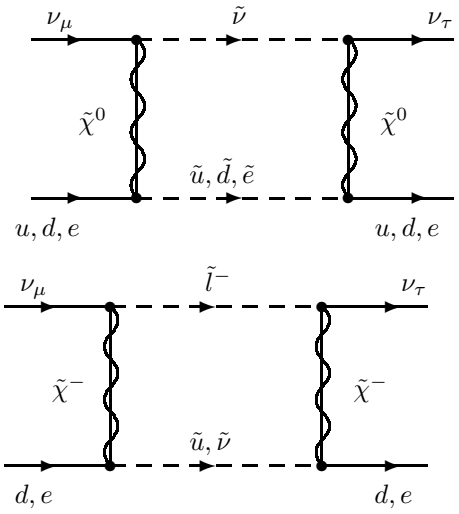

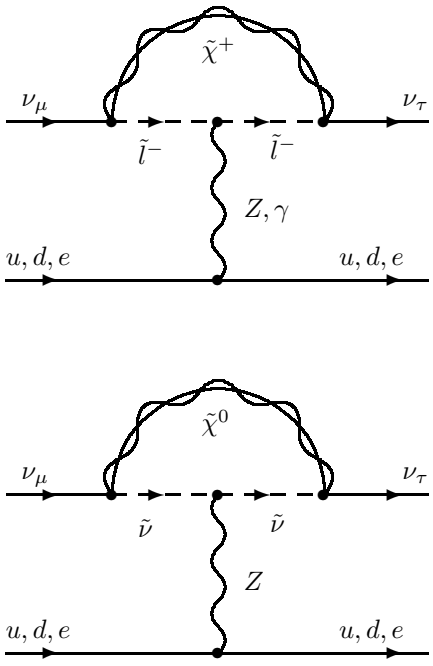

Finally Examples of LFV interaction in a detection process are depicted in the following diagrams.

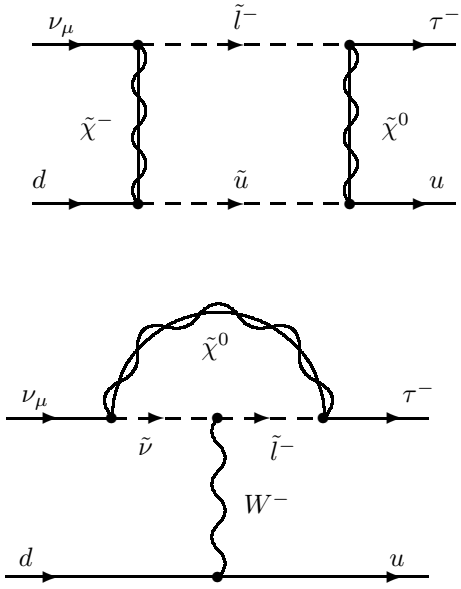

Amplitude of these graphs is estimated by mass insertion and dimensional analysis.

$$\begin{aligned}\mathcal{E} &\sim \frac{1}{16\pi^2}\frac{(\Delta m^2_{\tilde{L}})_{\alpha\beta}}{m^4_{\rm S}}g^4 \\ &\simeq -\frac{(6+a_0^2)}{(16\pi^2)^2}(f^\dagger_\nu f_\nu)_{\alpha\beta}\log\frac{M_G}{M_R}\ \frac{g^4}{m^2_{\rm S}} \qquad (25)\end{aligned}$$

and hence

$$\begin{aligned}\epsilon &= \frac{\mathcal{E}}{G_F} \sim -\frac{(6+a_0^2)}{(16\pi^2)^2}(f^\dagger_\nu f_\nu)_{\alpha\beta}\log\frac{M_G}{M_R}\ \frac{g^4}{m^2_{\rm S}G_F} \\ &\sim -\frac{(6+a_0^2)}{(16\pi^2)^2}(f^\dagger_\nu f_\nu)_{\alpha\beta}\log\frac{M_G}{M_R}\ g^2. \qquad (26)\end{aligned}$$

This implies that the amplitude can be $\mathrm{O}(10^{-4})$.

Moreover, since diagrams contribute coherently, as a whole ϵ can be larger by one order of magnitude. In fig.15 we plot the typical behavior of $\epsilon^s_{\mu\tau}$ in MSSM with right handed neutrinos.

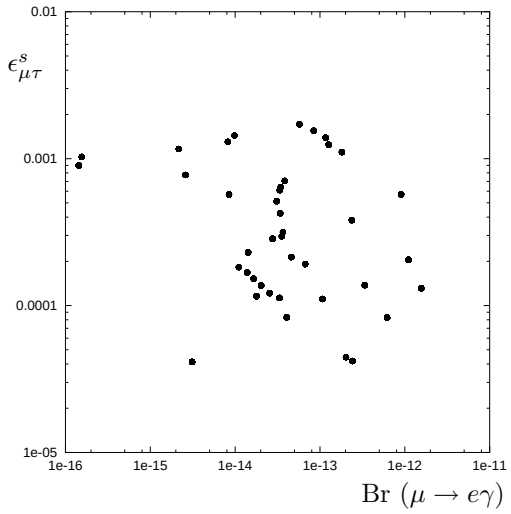

Figure 15. Example of Amplitude

5. Summary

Finally we summarize the content and give discussion. Motivated by MSSM with right-handed neutrinos, which is the most promising candidate for the physics beyond the standard model, we considered LFV in neutrino oscillation. This effect indeed can be large enough. If we have enough accuracy in mixing parameters, then we will have sensitivity for these couplings up to $\mathrm{O}(10^{-4})$. However if not, then we will still have the same sensitivity for several couplings and not for others. It depends on which oscillation mode we will observe. This is due to a strong correlation between some of LFV effect and mixing parameters. Because of the strong correlation, those effect may be hidden by the uncertainty of mixing parameters[17] or conversely we can not determine the mixing parameters precisely enough as we will expect[15].

The decay processes of muon and pion differ from each other. Therefore we might expect the case that new physics may affect only the decay of muon. The matter effect would be negligible for shorter baseline while for baseline longer than a thousand km it would be detectable. Thus to distinguish new physics effect from oscillation effect it is very useful to compare several modes.

There is another advantage the use of oscillation experiments for the determination of new physics effect. Experiment sensitivity is always limited by systematics, $\mathcal{S}$. The transition probability is given by $|\mathcal{A}+\epsilon|^2$, where $\mathcal{A}$ is oscillation amplitude. For direct measurement of the new physics, as $|\mathcal{A}| \ll |\epsilon|$, the reach of new physics is merely a square root of the systematics, $\mathcal{S}^2$. That is,

$$|\epsilon|^2 > \mathcal{S} \longrightarrow |\epsilon| > \sqrt{\mathcal{S}} \qquad (27)$$

In oscillation experiments the new physics effect enters with oscillation amplitude and hence the sensitivity on new physics may be raised. Indeed in oscillation experiments, for the new physics effect to be detectable, $\mathcal{A}\epsilon > \mathcal{S}$ is required. Thus we have the sensitivity reach,

$$\epsilon > \frac{\mathcal{S}}{\mathcal{A}}. \qquad (28)$$

The lower bound is alway smaller than the lower bound of the direct detection (27) since for the oscillation to be observed $\mathcal{A}^2 > \mathcal{S}$ is always expected:

$$\sqrt{\mathcal{S}} > \frac{\mathcal{S}}{\mathcal{A}}. \qquad (29)$$

Anyway we should keep in mind that there might be the new physics effect as there must be lepton flavor violating interactions.

REFERENCES

1. Super-Kamiokande Collaboration, S. Fukuda et al., Phys. Rev. Lett. **86**, (2001) 5651; 5656; SNO Collaboration, Q. R. Ahmad et al., Phys. Rev. Lett. **87** (2001) 071301 , ibid. **89** (2002) 011301 , ibid. **89** (2002) 011302 ,
2. Super-Kamiokande Collaboration, Y. Fukuda et al., Phys. Rev. Lett. **81** (1998) 1562; ibid. **82** (1999) 2644 ; ibid. **82** (1999) 5194.
3. KamLAND Collaboration, K. Eguchi et al., Phys. Rev. Lett. **90** (2003) 021802; CHOOZ Collaboration, M. Apollonio et al., Phys. Lett. **B466** (1999) 415 .
4. T. Yanagida, in *Proceedings of the Workshop on Unified Theory and Baryon Number of the Universe,* edited by O. Sawada and A. Sugamoto, Report KEK-79-18 (1979); M. Gell-Mann, P. Ramond and R. Slansky, in *Supergravity*, edited by D.Z. Freedman and P. van Nieuwenhuizen (North-Holland, Amsterdam, 1979)
5. F. Borzumati and A. Masiero, Phys. Rev. Lett. **57** (1986) 961.
6. J. Hisano, T. Moroi, K. Tobe, M. Yamaguchi and T. Yanagida, Phys. Lett. **B357** (1995) 579; J. Hisano, T. Moroi, K. Tobe and M. Yamaguchi, Phys. Rev. **D53** (1996) 2442.
7. J. Sato and K. Tobe, Phys. Rev. **D63** (2001) 116010.
8. L.M. Barkov *et al.*, Research Proposal to PSI, 1999. See the webpage: `http://www.icepp.s.u-tokyo.ac.jp/meg`.
9. MECO Collaboration, M. Bachman *et al.*, Proposal to BNL, 1997. See also `http://meco.ps.uci.edu`.
10. For example, see technical notes in the homepage of the PRISM project; `http://psux1.kek.jp/~prism`. See also the webpage of "Neutrino factory and muon storage rings at CERN"; `http://muonstoragerings.web.cern.ch/muonstoragerings/`
11. JHF-Kamioka project, Y. Itow *et al.*, hep-ex/0106019.
12. Neutrino Factory and Muon Collider Collab., D. Ayres *et al.*, physics/9911009; C. Albright *et al.*, hep-ex/0008064; D. Harris, *et al* eConf C010630 (2001) E1001 [hep-ph/0111030].
13. M.C. Gonzalez-Garcia, Y. Grossman, A. Gusso, and Y. Nir, Phys. Rev. **D64** (2001) 096006;
14. A. M. Gago, M. M. Guzzo, H. Nunokawa, W. J. C. Teves, and R. Zukanovich Funchal Phys. Rev. **D64** (2001) 073003;
15. P. Huber, and J. W. Valle, Phys. Lett. **B523** (2001) 151.
16. P. Huber, T, Schwetz, and J. W. F. Valle, Phys. Rev. **D66** (2002) 013006.
17. T. Ota, J. Sato, and N. Yamashita, Phys. Rev. **D65** (2002) 093015.
18. T. Ota and J.Sato, Phys. Lett. **B545** (2002) 367.
19. Y. Grossman, Phys. Lett. **B359** (1995) 141.
20. S. Bergmann, Y. Grossman, and E. Nardi, Phys. Rev. **D60** (1999) 093008 [hep-ph/9903517].
21. M. Koike, T. Ota, and J. Sato, Phys. Rev. **D65** (2002) 053015.
22. OPERA Collab., A. Rubbia *et al.*, Nucl. Phys. Proc. Suppl. **91** (2000) 223.
23. A. Bucno, M. Campanelli, S. Navas-Concha, and A. Rubbia, Nucl. Phys. **B631**(2002) 239;A. Rubbia, hep-ph/0106088.